Case Studies in Construction Materials 20 (2024) e03334

Contents lists available at ScienceDirect

Case Studies in Construction Materials

journal homepage: www.elsevier.com/locate/cscm

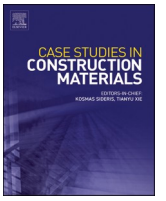

Degradation under cyclic wet-dry aging of full-scale high-workability concrete maximizing sustainable raw materials

Víctor Revilla-Cuesta [a,*], Javier Manso-Morato [a], Nerea Hurtado-Alonso [b], Amaia Santamaría [c], José T. San-José [d]

[a] Department of Civil Engineering, Escuela Politécnica Superior, University of Burgos, c/ Villadiego s/n, Burgos 09001, Spain
[b] Department of Construction, Escuela Politécnica Superior, University of Burgos, c/ Villadiego s/n, Burgos 09001, Spain
[c] Department of Mechanical Engineering, Escuela de Ingeniería de Bilbao, University of the Basque Country (UPV/EHU), Pl. Ingeniero Torres Quevedo 1, Bilbao 48013, Spain
[d] Department of Engineering in Mining, Metallurgy and Materials Science, Escuela de Ingeniería de Bilbao, University of the Basque Country (UPV/EHU), Pl. Ingeniero Torres Quevedo 1, Bilbao 48013, Spain

ARTICLE INFO

Keywords:
Steelmaking slag
Recycled concrete aggregate
High-workability concrete
Wet-dry performance
Linear thermal expansion coefficient
Hardened-property variations

ABSTRACT

Analyzing and validating the behavior of sustainable concrete mixes under near-realistic conditions is essential to advance their use. In this research, full-scale high-workability concretes, 0.5 m^3 in volume, containing maximum amounts of sustainable raw materials and their response in cyclic wet-dry tests are studied. The mixtures contained Electric Arc Furnace Slag (EAFS) and Recycled Concrete Aggregate (RCA) as aggregates, and Ladle Furnace Slag (LFS) and Ground Granulated Blast-furnace Slag (GGBS) as binders. Each mixture underwent 30 wet-dry cycles with temperature variations between 20 °C and 70 °C. Throughout the cycles, the internal-damage level was assessed through (increasing) weight measurements, (decreasing) ultrasonic-pulse-velocity readings, thermal strain, hardened-property variations, and flexural deformability. Overall, all the mixes underwent initial internal damage, attributable to both the thermal shock that increased with each cycle and the aging of the cementitious matrix, which in turn resulted in shrinking that reduced their thermal deformability. A linear thermal expansion coefficient of $1.6{\cdot}10^{-5}$ $°C^{-1}$ was adequate for safely estimating all the maximum thermal strains. Internal damage was less relevant with the use of EAFS and GGBS that led to fewer strength decreases, which were only 15–20% compared to 25–30% in the RCA mixes. However, the combination of EAFS and LFS increased flexural deformability after the test, which resulted in compliance under bending stresses that was two times higher than in the other mixes. Under those conditions, the joint use of EAFS and GGBS was the most recommendable multi-criteria and multi-purpose option where any change in concrete composition significantly affected behavior.

Abbreviations: ANOVA, analysis of variance; EAFS, electric arc furnace slag; GGBS, ground granulated blast-furnace slag; ITZ, interfacial transition zones; LFS, ladle furnace slag; MIP, mercury intrusion porosimetry; MCDM, multi-criteria decision-making; RCA, recycled concrete aggregate; SCC, self-compacting concrete; UPV, ultrasonic pulse velocity.

* Corresponding author.
E-mail address: vrevilla@ubu.es (V. Revilla-Cuesta).

https://doi.org/10.1016/j.cscm.2024.e03334
Received 23 February 2024; Received in revised form 24 April 2024; Accepted 22 May 2024
Available online 23 May 2024

1. Introduction

Concrete is the most widely used material in both the building and the civil-engineering sectors. Among the many applications of concrete [1], perhaps its most widely known forms are *par excellence* beams and columns [2]. However, its range of application is much wider. Concrete can also be used for pavement construction [3,4], urban-furniture elements such as benches and curb stones [5], and large components, either in mass or reinforced, such as retaining walls and pipes [5,6]. In all these applications, except when used in an indoor environment, concrete is exposed to cyclic wet-dry conditions [7], *i.e.*, periods of both rain and solar heating [8]. The behavior of any type of concrete under such environmental conditions must be monitored, not only to check for potential concrete-reinforcement corrosion [9], but also to foresee any changes that these processes can cause in the concrete performance [10]. A good option to evaluate this behavior is through laboratory tests that simulate the wet-dry conditions to which concrete can be exposed [7,11]. In these tests, concrete is subjected to more extreme exposure conditions than those it undergoes when in service, which enables its behavior to be further verified [11].

Fresh-state workability for suitable usage is a very important quality in any concrete design. High workability has great advantages for many of the above-listed applications [12,13]. On the one hand, the concrete arrives in better condition following transport from the point of manufacture to the site. It will always lose workability during transport, yet if its initial workability is high, then its final workability will not be far off that state [14]. On the other hand, improved workability eases concreting, as it facilitates pumping and formwork filling, and reduces any need for vibration [15]. In addition, the smoother and less porous finish lends a better appearance to the concrete surface [16]. There is therefore a growing trend towards S4 slump class concretes, with very high slumps between 160 and 210 mm, as *per* EN 206 [17]. However, the maximum expression of a high-workability concrete is Self-Compacting Concrete (SCC), which is able to fill any type of formwork without vibration, as long as it is correctly designed [18,19]. The most widely used precast-concrete is therefore SCC [20].

The extraction of natural aggregates from quarries and gravel pits for use in concrete production causes worrisome environmental impacts [21] and depletes natural resources [22]. It has prompted intensive research into the performance of concrete containing sustainable aggregates, such as Electric Arc Furnace Slag (EAFS), a residue from the smelting of steel scrap [23–25], and Recycled Concrete Aggregate (RCA) from the crushing of out-of-use concrete [26,27]. Concrete with adequate workability and strength for all the above-mentioned applications can be obtained with these two types of aggregate through a proper mix design [1,28]:

- Outdoor weathering (and therefore aging) prior to use is essential to ensure the dimensional stability of EAFS [29]. In addition, increasing the fines content in the concrete mix is necessary to create a cement paste that can drag dense EAFS particles within fresh concrete, thus achieving adequate workability and even self-compactability [22,28].
- RCA is obtained by crushing concrete elements, so it has hydrated mortar in its composition, either as fine particles [30] or adhered to the natural-aggregate particles [31]. It means that RCA has high water-absorption levels [32]. Increasing the water-to-cement ratio will therefore maintain concrete workability when using RCA [26] to the point where SCC can even be developed [33]. Nevertheless, the increase in water content should not be excessive, so as not to increase the effective water-to-cement ratio. In doing so, any further decrease in strength other than because of the increase of concrete porosity as a result of RCA additions was avoided [7,34].

Ladle Furnace Slag (LFS), a by-product of steel refining, can be simultaneously used as an aggregate and supplementary cementitious material [35], provided its expansiveness is kept under control [36]. The possible expansiveness of concrete after additions of EAFS and LFS, and its higher porosity after additions of RCA usually worsen the behavior of concrete under wet-dry aging [7,11,37].

The manufacture of Portland cement also causes major environmental impacts, because of high CO_2 emissions [38]. Thus, the feasibility of using waste, such as Ground Granulated Blast-furnace Slag (GGBS), in replacement of cement has also been analyzed in scientific research [39,40]. This residue comes from the grounding of blast-furnace slag and hardens when mixed with water, although it provides lower strength than ordinary Portland cement [24]. Its low grinding fineness hinders aggregate dragging and reduces concrete workability [41], but also creates a compact internal micro-structure that limits the entry of damaging external agents within the concrete [42]. Traditionally, it has therefore been used for soil stabilization [43] and in concrete components under low mechanical stress and exposed to marine environments [44]. However, it has more recently been proven that suitable structural components can be developed using this binder, provided that the dosage is correctly adjusted, so as to compensate for the aforementioned effects [45,46]. GGBS generate compact micro-structures within concrete, so that it performs better under cyclic wet-dry tests [47]. Its addition can even compensate for the detrimental effects of other sustainable raw materials [11].

Moving towards the use of concretes with high contents of sustainable raw materials is essential to minimize the high environmental impact of conventional-concrete production processes [21,38]. Their application requires the production of concrete on an industrial scale, *i.e.*, in large volumes [20]. It is therefore necessary to analyze the behavior of full-scale concrete made with such raw materials. Nevertheless, concrete behavior has mainly been studied at laboratory scale (simultaneous production of 80-liter batches), where the proportion of the components and their interaction is perfectly controlled [48]. Large-scale production involves slightly different mixing conditions that also need analyzing, a novel aspect that has not yet been addressed in scientific research as *per* the author's knowledge.

In this paper, the cyclic wet-dry behavior of high-workability concrete samples with high contents of sustainable raw materials is studied for full-scale production (volumes of 0.5 m^3). Pumpable concrete with EAFS, GGBS, and LFS, and SCC with RCA, GGBS, and LFS were designed, based on previous studies of the authors [15,28,49]. The mix specimens were subjected to cyclic wet-dry tests, evaluating all aspects of concrete behavior that these exposure conditions affect: internal damage, thermal strain, hardened-property

variations, and deformability. The objective and novelty of the study consisted in arriving at a clear definition of the effects of exposure to wet-dry cycles in a full-scale concrete produced with high contents of sustainable raw materials. Those effects were studied on mixtures similar to those used in the industrial field (high workability, adequate strength, and large-volume production). Establishing a clear framework for analyzing their behavior will, it is hoped, advance the widespread use of highly sustainable concrete mixes.

2. Materials and methods

2.1. Raw materials

2.1.1. Cement, water and admixture

Two different cement types, both standardized according to EN 197–1 [17], were used in this research: CEM I 52.5 R and CEM III/A 42.5 N. The first one, ordinary Portland cement, with a density of 3.15 kg/dm^3 and a Blaine specific surface (EN 196–6 [17]) of 450 m^2/g, containing 90% clinker, is commonly used in structural concrete [16]. The second cement containing 47% GGBS yields lower compressive strengths [45], as its marking indicates. The presence of that waste also implies a slightly lower density than ordinary Portland cement (3.05 kg/dm^3) and a higher specific surface (540 m^2/g) [41].

Drinking water was used to prepare the mixes. Two admixtures were also employed, in order to reach the high-workability goal while ensuring adequate strength [50]. One improved the flowability of the mixes (viscosity-regulator admixture), while the other reduced the overall water demand (plasticizer admixture) [41]. According to the experience of the authors [7,41], high workability can be reached with amounts of plasticizer that are twice the amount of viscosity regulator.

2.1.2. Aggregates

A waste management company supplied the EAFS after cooling of the raw slag recovered from the electric arc furnace, magnetic removal of metallic elements, crushing, and weathering. Three different fractions (0–4 mm, 4–12 mm, and 12–20 mm) were used, in order to adjust the global gradation through their continuous granulometry (Fig. 1a). In addition, the maximum aggregate size was suitable for the development of pumpable concrete [15]. Their physical properties, among which their especially notable high densities, are detailed in Table 1.

The RCA consisted of crushed precast-concrete components whose concrete strength was at least 45 MPa. Geometrical and aesthetic defects had led to the rejection of these components after casting. The components could then be sieved and crushed to manufacture RCA with two fraction sizes: 0–4 mm and 4–12.5 mm. RCA particle sizes were continuous (Fig. 1b) and the maximum aggregate size was adjusted for SCC production [7]. Among the physical properties (Table 1), the much higher water-absorption levels of RCA than natural aggregate were noteworthy [32].

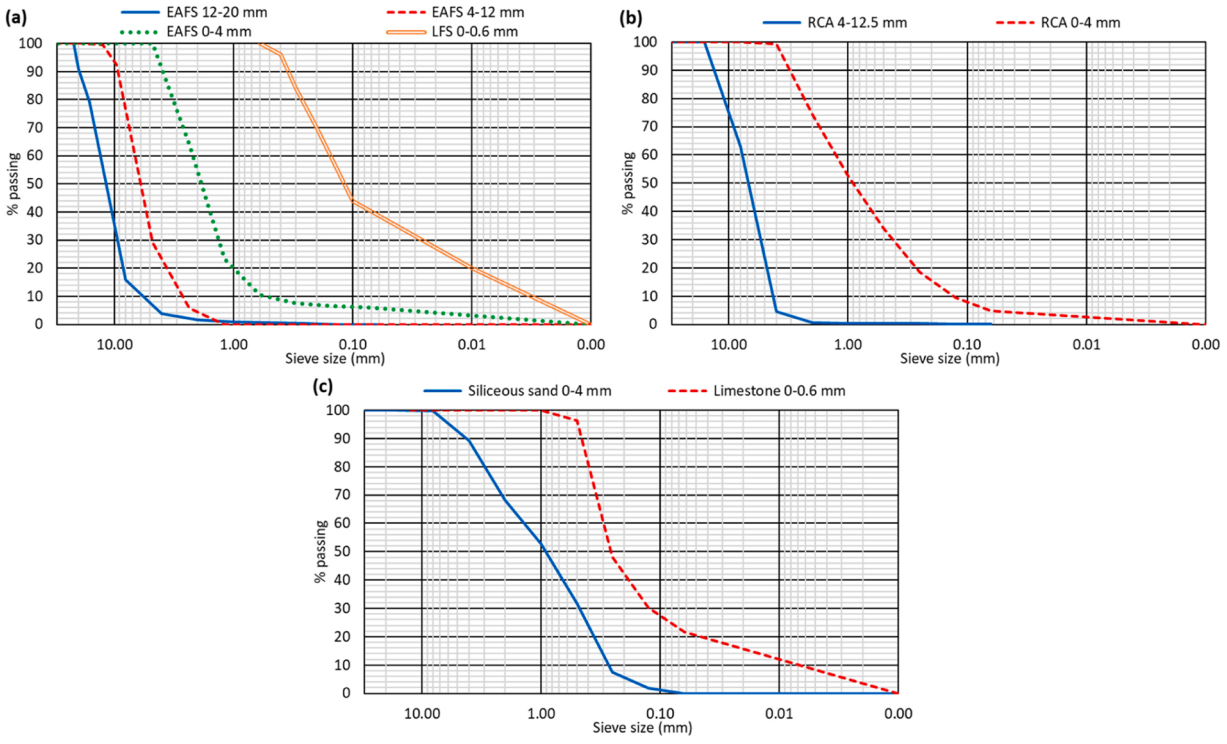

Fig. 1. Gradation of the aggregates: (a) steelmaking slag; (b) recycled concrete aggregate; (c) natural aggregates.

Table 1
Aggregate density and water-absorption levels.

Aggregate	SSD density (kg/dm^3)	Water absorption (% wt.)
EAFS 12–20 mm	3.42	2.12
EAFS 4–12 mm	3.42	2.12
EAFS 0–4 mm	3.42	2.12
LFS 0–0.6 mm	3.03	-
RCA 4–12.5 mm	2.42	6.25
RCA 0–4 mm	2.37	7.36
Siliceous sand 0–4 mm	2.58	0.25
Limestone 0–0.6 mm	2.65	0.60

SSD: Saturated surface dry.

The LFS was of a grayish powdery appearance, as is common in this waste [36]. The LFS received in the laboratory (fraction 0–2 mm) was sieved to obtain the 0–0.6 mm fraction, with the objective of it simultaneously functioning both as a supplementary cementitious material and as aggregate fines [35]. A very high fines content in the LFS is necessary to achieve this performance (Fig. 1a). LFS density was found to be around 3 kg/dm^3 (Table 1).

Finally, two natural aggregates were used. On the one hand, siliceous sand (0–4 mm) was used to complete the fine-aggregate fraction (0–4 mm) in the RCA mixes, because 100% fine RCA was not recommendable on the basis of previous research [49]. On the other hand, limestone fines (0–0.6 mm) from quarry waste with calcite contents higher than 95% were used. Those fines were used to improve the workability of the EAFS mixes, because they contribute to the formation of a compact cement paste [28] and provide the necessary fines content for self-compactable RCA mixes [41]. Their particle size is shown in Fig. 1c and their physical properties in Table 1, both of which reflect conventional values [51,52].

More information on all the aggregates used for the mixes described in this paper can be found in a previous paper linked to the same research line of the authors [48].

2.2. Mix design

The mixes were designed based on previous findings from authors' studies on the use of EAFS and RCA in concrete [28,49]. The design maximized waste usage and yielded mechanical behavior suitable for structural use, while increasing sustainability. The basic design aspects are described in this section and a detailed description can be consulted in a previous article of the authors [48].

The mixes with EAFS were designed as pumpable concretes, *i.e.,* having an S4 slump class (slump of 185±25 mm) as *per* EN 206 [17], which is the most suitable workability for EAFS concrete. That sort of slump class facilitates placement and, at the same time, reduces the risk of segregation within the fresh mixes that the high density of EAFS can provoke [53]. All the aggregate in these mixes was EAFS, except for the finest fraction, which was composed of 0–0.6 mm limestone fines. The fines content of EAFS is very low, so it is necessary to add aggregate fines, which also hinder EAFS segregation, thereby favoring adequate mix workability [28,53]. Saturation of the EAFS also further improved workability [24]. Two mixes with EAFS were prepared, both containing 300 kg/m^3 of binders, each of a different nature. One mix incorporated 88% CEM I and 12% LFS, it having been demonstrated that the latter amount can reduce the use of ordinary Portland cement [35]. The other mix was made with 100% CEM III/A. Both mixes shared the same water-to-binder ratio of 0.40 and an admixture content of 1.3% wt. of the binder mass, which are standard values according to the most common concrete-dosage methods [51,52].

Two other SCC mixes with conventional slump flows (650±100 mm) [14] were prepared with RCA, as adequate performance of this type of concrete has been demonstrated in previous studies when using that sustainable aggregate [33,41]. The binder and water-content guidelines were the same as for the two EAFS mixes. Thus, both incorporated 300 kg/m^3 of binder, one 88% CEM I and 12% LFS and the other 100% CEM III/A, and had a water-to-binder ratio of 0.40. The whole coarse (4–12.5 mm) aggregate fraction was RCA, while half of the fine (0–4 mm) fraction was RCA and the other half was siliceous sand. Previous studies have shown that the use

Table 2
Mix composition (kg/m^3).

Mix	*IS*	*IIIS*	*IRC*	*IIIRC*
CEM I 52.5 R	258	0	258	0
CEM III/A 42.5 N	0	300	0	300
LFS 0–0.6 mm	42	0	42	0
Water	120	120	120	120
Admixtures	3.9	3.9	6.0	6.0
EAFS 12–20 mm	450	450	0	0
EAFS 4–12 mm	610	610	0	0
EAFS 0–4 mm	660	660	0	0
RCA 4–12.5 mm	0	0	580	580
RCA 0–4 mm	0	0	600	600
Siliceous sand 0–4 mm	0	0	300	300
Limestone 0–0.6 mm	640	640	360	360

of 100% fine RCA 0–4 mm is not recommendable, as those fines weaken the mechanical behavior of the concrete [49]. The RCA was pre-saturated to compensate for its high-water absorption [32] and to ensure adequate self-compactability. The admixture content was 2.0% wt. of the binder mass and limestone (0–0.6 mm) was added to achieve the necessary content of aggregate fines [41].

The mixes were labelled with a Roman numeral, *I* or *III*, which referred to the type of cement in use. An *S* or *RC* was then placed after the numeral, if the mix incorporated either EAFS or RCA, respectively. Thus, for example, the *IIIS* mix incorporated CEM III/A and EAFS. All the mix compositions and the aspects discussed in this section are shown in Table 2.

2.3. Experimental plan

The mixes were manufactured on a large scale, in a volume of 0.5 m^3, with the objective of analyzing the mix behavior when produced in industrial volumes [20]. After mixing, the slump test (EN 12350–2 [17]) was used to evaluate concrete workability in the EAFS mixes, and the slump-flow (EN 12350–8 [17]) and 3-bar L-box (EN 12350–10 [17]) tests were used to evaluate the workability of the RCA mixes. Beams were then poured, together with different types of specimens to assess the mechanical properties, porosity, and cyclic wet-dry behavior of the mixes. The specimens remained in the laboratory environment for the first 24 hours and were subsequently stored in a humid chamber (90±5% relative humidity and 20±2 °C temperature) until the different test ages. All the research results are presented as average values of three different test specimens.

A comprehensive analysis of the mechanical performance and durability has previously been conducted to evaluate the concrete properties [48]. However, the relevant properties that are related to the aspects discussed in this paper for the cyclic wet-dry test were as follows:

- Mechanical performance was evaluated at a set age of 28 days. Hardened density (EN 12390–7 [17]) was measured in 10x10x10-cm cubic specimens, compressive strength (EN 12390–3 [17]) on 10×20-cm cylindrical specimens, and flexural strength (EN 12390–5 [17]) on 7.5×7.5×27.5-cm prismatic specimens. The load-deflection curves in the flexural-strength tests were also recorded.
- At an age of 180 days, Mercury Intrusion Porosimetry (MIP) tests were conducted using an Autopore IV 9500 apparatus working up to a pressure of 33,000 psi (227.5 MPa) to evaluate the internal porosity of each specimen. In addition, concrete skin permeability and concrete water absorption were evaluated in 10x10x10-cm cubic specimens in two different ways. After conditioning as *per* UNE 83966 [54] and weighing, three specimens were immersed in water at room temperature (20±2 °C) for 24 h following the indications of UNE 83980 [55], and another three in boiling water (temperature of 70±2 °C) for 24 h as *per* ASTM C642 [56]. After the tests, all the specimens were weighed. The percentage weight differences determined the water-absorption levels of the mixes.

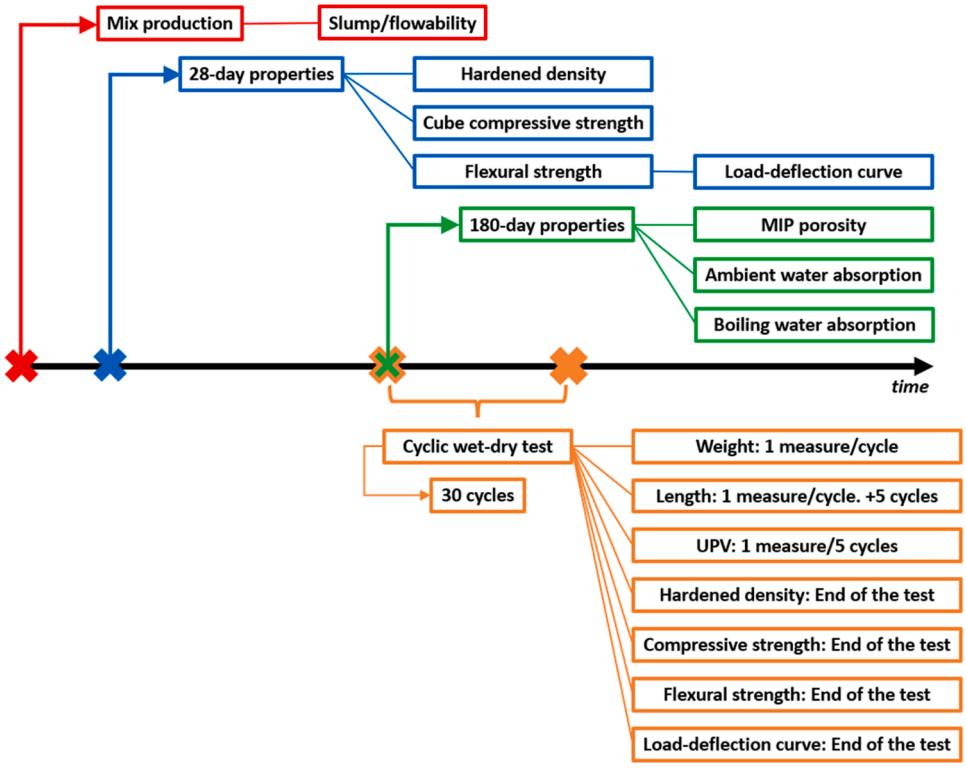

Fig. 2. Experimental plan.

At the same age of 180 days, the cyclic wet-dry test was also started, which was performed on both 10x10x10-cm cubic specimens and 7.5×7.5×27.5-cm prismatic specimens. The specimens were firstly conditioned in terms of humidity according to UNE 83966 [54]. Subsequently, the specimens were subjected to 30 wet-dry cycles, number of cycles determined by adapting the standard ASTM D559 [56] and by similarity with previous research by the authors [11,57]. Each cycle consisted of immersion in water at room temperature (20±2 °C) for 16 h and then oven drying at 70±2 °C for 24 h. Five aspects of the concrete were evaluated:

- Both types of specimens were weighed at the end of each cycle to evaluate the evolution of porosity and internal damage [11], a dry weight after 8 h of oven-drying being therefore always measured. The porosity values obtained through MIP and water-absorption tests were used as a reference to analyze the performance of the mixes.
- Ultrasonic Pulse Velocity (UPV) was measured every 5 cycles on both types of specimens, to quantify the extent of internal damage within the concrete [7].
- The length of the prismatic specimens was also measured after each cycle using a comparator with a precision of 1 μm, to monitor the evolution of the thermal deformability [15], through which the thermal expansion coefficient of the mixes could be calculated [58]. Furthermore, the specimens were left at room temperature (20±2 °C) for a time corresponding to 5 cycles after the end of the test to analyze the remaining strain of the mixes [15].

- The hardened density according to EN 12390–7 [17] and the compressive strength as *per* EN 12390–3 [17] of the mixes were obtained after the cyclic wet-dry tests on cubic specimens. Flexural strength as *per* EN 12390–5 [17] was determined by testing the prismatic specimens. These results were compared with the 28-day results, to analyze the extent of strength loss after the cyclic wet-dry test [7,11].
- Finally, the load-deflection curves of the concrete mixes were continuously recorded during the flexural-strength test. Both the load and deflection were measured by the testing press. The deflection was determined by recording the displacement of the loading piston. In that way, concrete deformability after the cyclic wet-dry test could be assessed and compared with that at 28 days [53].

For clarity, the experimental plan followed in this study and its temporal distribution are shown in Fig. 2. The experimental results of the wet-dry test were also statistically evaluated using an ANalysis Of VAriance (ANOVA) to determine their significance. In addition, two Multi-Criteria Decision-Making (MCDM) algorithms, TOPSIS and PROMETHEE, were applied to define the optimal raw material combination for the concrete to withstand the effects of cyclic wet-dry conditions [41].

3. Reference results and discussion

3.1. Fresh performance

The results of the fresh-state tests are reported in Table 3. A much more detailed analysis of the fresh behavior of these concrete mixtures can be found in a previous paper of the authors [48].

The mixes with EAFS achieved the S4 slump class requirement specified in EN 206 [17]. In fact, the CEM I mix showed the highest slump value within that class. So, despite the high density of EAFS, which hinders particle dragging within the fresh cement paste [24], the adjustment of the fines content with additions of limestone fines (0–0.6 mm) formed a dense paste that met the slump requirements [28]. All the aspects measured for the RCA mixes were suitably adjusted to an SCC. Thus, the RCA mixes showed a SF1-SF2 slump-flow class, a VS2 slump-flow-viscosity class, and a PA2 passing-ability class as *per* EN 206 [17]. RCA is difficult to drag within the fresh cement paste, because of its angular and irregular shape and its high water-absorption levels [27,33]. Therefore, high workability was achieved, because of the precise adjustment of the content of coarse RCA and water in the concrete dosage.

The use of CEM III/A reduced workability, regardless of the type of concrete and aggregate. So, the EAFS-mix slumps saw reductions of 45 mm, while the slump flows of the RCA mixes fell 120 mm. Furthermore, there was a 20% increase in the slump-flow viscosity of the SCC mixes and their blocking ratio was the lowest permissible value [33]. The grinding fineness of the GGBS found in that cement type is lower than in ordinary Portland cement [47], so its aggregate particle dragging capability is reduced [42]. If an aggregate that does not favor concrete workability, such as EAFS or RCA, is also used, it is further aggravated [41]. However, it should be noted that in the mixes of this study, the established workability targets were achieved despite the combination of GGBS with sustainable aggregates.

Table 3
Fresh performance.

Mix	Slump (mm)	Slump flow (mm)	Slump-flow viscosity t_{500} (s)	3-bar L-box blocking ratio
IS	210	-	-	-
IIIS	165	-	-	-
IRC	-	700	4.0	0.9
IIIRC	-	580	4.8	0.8

3.2. Mechanical performance

The 28-day mechanical properties of the mixes are detailed in Fig. 3. All values were found to be suitable for use of the concrete mixes in structural applications, as can also be noted from the more detailed descriptions given elsewhere [48]. The results of the load-deflection curves are presented in later sections for comparison with those obtained after the cyclic wet-dry test.

In relation to hardened density (Fig. 3a), the EAFS mixtures, at around 2.7 kg/dm^3, had higher densities than the RCA mixes, which presented values of 2.1–2.2 kg/dm^3. The explanation is found in the higher density of EAFS, as reported in the scientific literature [5, 22], and can be observed in the particular case of this study in Table 1. In addition, the higher fine-aggregate content and the higher proportions of occluded air after the inclusion of admixtures within SCC makes it less dense than pumpable concrete [20,59]. The additions of GGBS hardly modified the densities of the EAFS mixes, although the densities of the SCC mixes with RCA were reduced, in all likelihood as a result of worsening interactions between both wastes [60], which increased total porosity [48], as confirmed in the MIP test (Fig. 4a), detailed in the following section.

In terms of strength, the EAFS mixes performed better than the RCA mixes, mainly on account of the following two aspects. On the one hand, the EAFS formed dense and strong Interfacial Transition Zones (ITZ) [60], which were weaker in the RCA concretes because of the adhered mortar [1]. On the other hand, the higher content of limestone 0–0.6 mm in these mixes resulted in a more compact cementitious matrix [53]. The fact that the RCA mixes were SCC, with a lower coarse aggregate content that weakened the resistant concrete skeleton, should also be noted [33]. The effect of CEM III/A on this behavior was different for both sustainable aggregates. It never affected the compressive strength of the EAFS mixes, although it slightly increased their flexural strength (increase of 0.15 MPa). In contrast, GGBS worsened all properties in the RCA mixes, resulting in decreases of 10–15% across the board. A deteriorating performance that may be linked to the increase in total porosity associated with that alternative binder [11,48].

3.3. Porosity

Concrete mix porosity was evaluated using MIP and water-absorption tests (Fig. 4), as detailed in greater detail elsewhere [48]. Fig. 4a shows the results of porosity obtained by MIP:

- The EAFS mixes had lower porosities in relation to total porosity than the RCA mixes when using the same cement type. A behavior that was partially attributable to the higher amount of admixture in SCC compared to pumpable concrete, which resulted in higher air content [59]. In addition, the aggregate type also affected porosity levels. The presence of adhered mortar in the RCA weakened the ITZ, leaving it more porous [31]. Likewise, the worse affinity of the fine RCA with cement also increased porosity [61]. The porosity levels of CEM III/A that contained GGBS increased, quite noticeably when combined with RCA (6% in absolute terms). Those total porosity results largely explain the values of the different mechanical properties (Fig. 3) [15].
- Effective porosity can be defined as the porosity that determines concrete permeability [62]. It is therefore formed of pore sizes that are larger than 60–70 nm [62]. The effective MIP porosities shown in Fig. 4a are obtained when the pore volumes smaller than

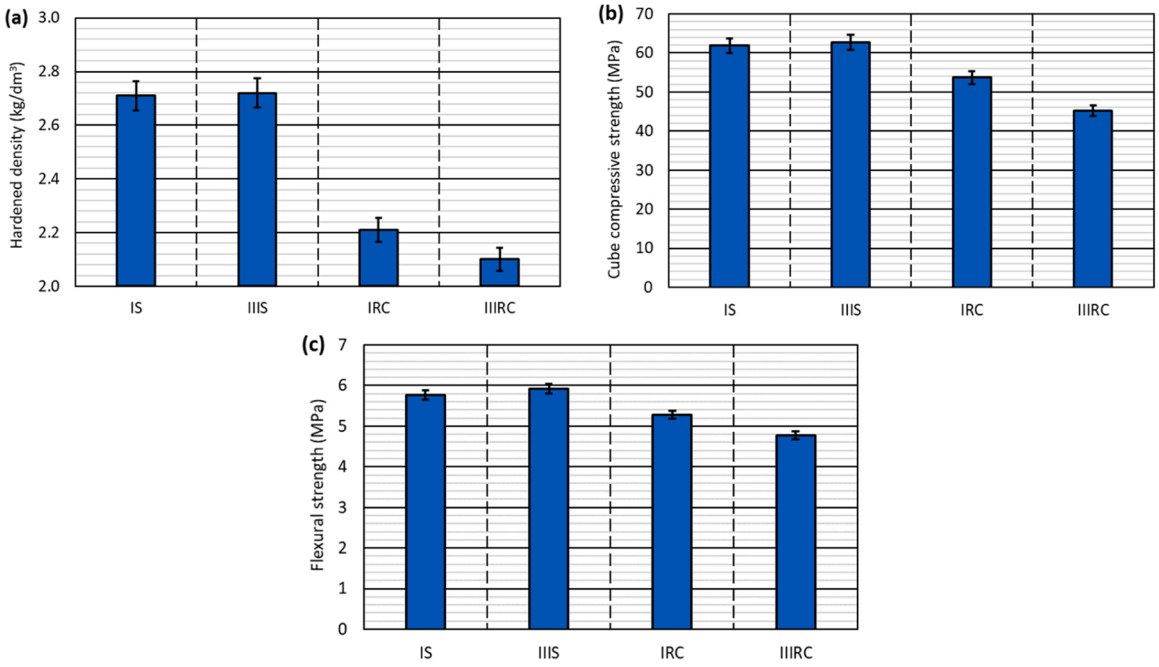

Fig. 3. 28-day hardened properties: (a) hardened density; (b) cube compressive strength; (c) flexural strength.

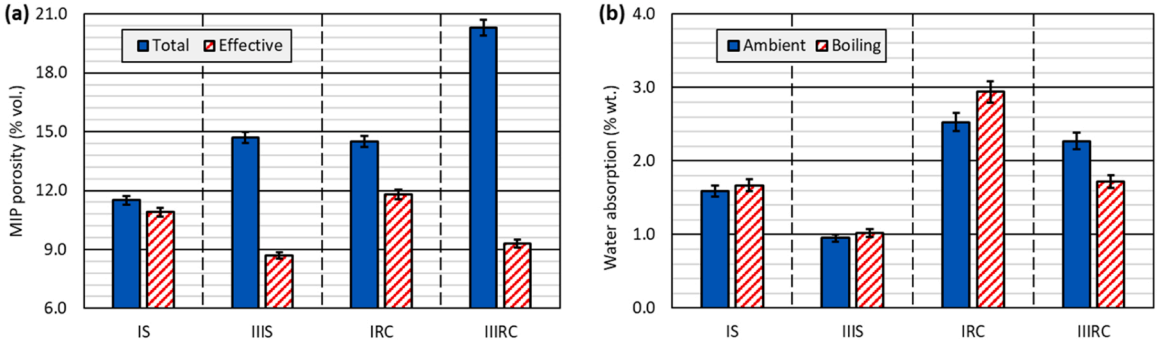

Fig. 4. 180-day porosity performance: (a) MIP porosity; (b) full-immersion water absorption.

70 nm are subtracted from total porosity. These results show that the effect of aggregate type on effective porosity was the same as on total porosity. Nevertheless, the effect of CEM III/A was quite the opposite, as it increased the number of pores smaller than 70 nm, which augmented total porosity and decreased effective porosity. Thus, GGBS formed more compact micro-structures against permeability, as already found in other studies [42,60], which explains the good performance of GGBS concrete undergoing cyclic wet-dry processes [47].

The more compact structure that can withstand permeability is reflected in the water-absorption results, detailed in Fig. 4b, which were coincident with the effective-porosity trends. Thus, additions of RCA meant that the concrete absorbed more water than when EAFS was added, while water absorption in the GGBS mixes fell 0.5% in absolute terms. Unlike standard concrete behavior, water transport and mechanical properties behaved in quite the opposite way [10,15]. In general, water absorption in boiling water was minimally higher than in water at ambient temperature, which the partial decomposition of primary ettringite that occurs at that temperature might help explain [62]. Furthermore, the greater sensitivity of RCA to high temperatures may have resulted in micro-cracking and internal damage to the concrete and, in consequence, higher levels of water absorption [58], as found in the *IRC* mix. However, this initial internal damage was limited in the *IIIRC* mix due to the compact micro-structure created by GGBS [62], as previous studies have recorded water absorption in SCC of up to 1.5% less in absolute value with the addition of GGBS [15,63].

4. Wet-dry-test results and discussion

The overall results of all the concrete mixes obtained during the cyclic wet-dry test are reported in Table 4. A detailed analysis of them all is provided in the following sections. No differences were found among the mixtures regarding the external aspect of the concrete specimens after the test, as no visible signs of damage were found in any of them, except for some superficial chips in some specimens (Fig. 5).

4.1. Weight variation

Weight variations due to water absorption throughout the wet-dry test are shown in Fig. 6 where the variations and the influence of the mix composition on weight gains can be analyzed.

Table 4
Properties of the mixes during the cyclic wet-dry test (average values).

Property		*IS*	*IIIS*	*IRC*	*IIIRC*
Weight	**Initial value (g)**	4177.4	4188.9	3376.7	3192.2
	Final value (g)	4333.4	4323.5	3548.7	3347.0
	Variation[a] (%)	+3.73	+3.21	+5.09	+4.85
UPV	**Initial value (km/s)**	3.92	3.68	3.77	3.54
	Final value (km/s)	3.79	3.56	3.57	2.29
	Variation[a] (%)	-3.42	-3.35	-5.43	-7.00
Thermal strain	**Value after the test (mm/m)**	0.532	0.416	0.745	0.645
	Remaining value (mm/m)	0.332	0.233	0.549	0.451
Hardened density	**Value after the test (kg/dm^3)**	2.73	2.74	2.24	2.12
	Variation[b] (%)	+0.74	+0.74	+1.36	+0.95
Compressive strength	**Value after the test (MPa)**	47.4	49.5	37.8	31.0
	Variation[b] (%)	-23.4	-21.05	-29.61	-31.57
Flexural strength	**Value after the test (MPa)**	4.69	4.96	3.87	3.42
	Variation[b] (%)	-18.6	-16.22	-26.70	-28.30

[a] Variations between the values at the beginning of the test (initial values) and at the end of the test (final values).
[b] Variations between the values obtained after the cyclic wet-dry test and the values at 28 days (Fig. 3).

Fig. 5. Specimen of the *IIIS* mix after the cyclic wet-dry aging.

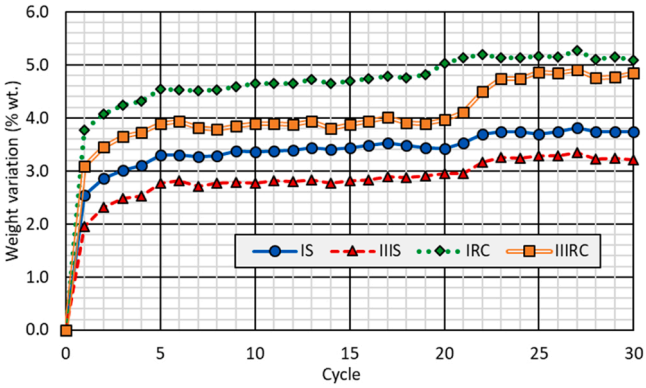

Fig. 6. Weight variation throughout the cyclic wet-dry test.

Weight variations throughout the test were divided into four stages: first cycle, progressive weight increase, stabilization phase, and slower weight increase. These stages were similar for all the mixtures, regardless of their composition.

- First, it should be noted that the water absorption, or the weight increase of each mixture after the first cycle was between 50% and 100% higher than in the water-absorption tests (Fig. 4b): the lower the water absorption of the mix, the greater the difference. A behavior that internal damage within the concrete during this first cycle of the test might explain [10], which led to micro-cracking and perhaps a small increase in the size of some micro-pores [64]. In the first cycle, the consequences of component deformability and responses to the sudden change of environment (thermal shock) [11] affected the concrete mixes.
- After the first cycle, the weight of the mixes continuously increased until the fifth cycle. It seems that the damage in the mixtures during these first wetting and drying cycles progressively increased during the initial phase [10].
- From the fifth cycle onwards, the weight remained practically constant, showing practically null variations of at most 0.1% in absolute terms, which are thought to be because of the experimental variability of the results when conducting the test. The mixtures showed an adaptation to these cyclic environmental conditions and micro-cracking never increased until approximately cycle 20–21.
- From cycle 20–21, the mixtures showed weight increases of approximately 0.2% in absolute terms. The slower weight increase may be attributable to specimen aging [7], and perhaps to the partial decomposition of primary ettringite [62], which might have weakened the cementitious matrix. The *IIIRC* mix showed a much higher weight increase than the other mixtures, 0.5% in absolute terms, which more pronounced aging might explain, because of the lower quality of its cementitious matrix [15] and its worse mechanical properties (Fig. 3).

The weight difference between the mixes was practically the same throughout the entire test, with the exception of the behavior shown by the *IIIRC* mix starting at cycle 20. Thus, the composition of the mixes had no great effect, neither on the evolution of weight nor, in consequence, on the evolution of the internal damage throughout the wet-dry test. However, the mix composition conditioned the value of the weight increase. Scientific literature has revealed that EAFS concrete has the same water-absorption levels as

conventional concrete [5,53], as happened in this research. The EAFS mixtures therefore showed a lower weight increase than the RCA mixtures, as RCA further increased concrete porosity due to the adhered mortar that increased ITZ porosity [31], and due to the worse affinity of fine RCA when mixed with cement [61]. In addition, the higher admixture content of SCC gave it higher porosity levels than the pumpable concrete [50]. Moreover, the use of CEM III/A with GGBS reduced water absorption, creating a more compact micro-structure with smaller pore sizes [42]. A higher level of porosity implied greater internal damage in the mixes when subjected to cyclic environmental variations [34], so the weight-evolution trends shown by the mixes were coincident with the results of the water-absorption tests and the MIP effective porosities (Fig. 6).

4.2. UPV evolution

UPV readings of the mixes were recorded every five cycles for an indirect measure of their internal-damage levels [65]. Both the initial and the final values, as well as their variations are detailed in Table 4. The UPV trends throughout the whole cyclic wet-dry test are represented in Fig. 7.

Although the percentage UPV variations compared to other UPV concrete test results were very small [11,65], they coincided with the stages related to weight evolution that have been described. In the first five cycles, a sharp drop in UPV values, ranging from 2.5% to 5.0%, was detected, following the damage that the mixes underwent in the first five cycles [37]. Subsequently, the UPV readings remained approximately constant until cycle 20. UPV measurement oscillations, which are inherent to that property, were observed in the CEM I mixtures [66]. However, small decreases of at most 0.5% were noted in the CEM III/A mixes, which showed more continuous patterns of internal damage linked to the use of that cement type, which had not been detected in the weight-related variations. Finally, clearly lower UPV readings from cycle 20 onwards were noted in all the concrete mixes as a consequence of the delayed internal damage to the mixes [7,8]. A drop that was 0.2–0.3% in all mixes, except in the *IIIRC* mix, in which it reached a value of 2.5%, coherent with the weight variations and the combination of aging and the worse quality of its cementitious matrix that had caused high levels of internal damage in the mix [15].

The modifications to the mix compositions and their effects were approximately coincident with their weight variations (Fig. 6) and effective-porosity trends (Fig. 4b). Thus, on the one hand, higher internal damage and lower UPV readings were observed in the RCA mixes than in the EAFS mixes. On the other hand, the mixtures with CEM III/A showed smaller and lower initial UPV readings, although the effect of their more compact micro-structure [42] was not as clear. The explanation is that as from cycle 20, the lower UPV readings were practically equal in the EAFS mixes regardless of the cement type, while in the RCA mixes the UPV readings were lower in the *IIIRC* mix. The compact micro-structure that could be clearly detected in the initial UPV readings limited water penetration, as the micro-cracking had affected small pore sizes during the application of the cyclic wet-dry cycles [15,60].

4.3. Thermal-strain evolution

The specimens tested during the wet-dry test increased in length when moved from water at 20±2 °C to an oven at 70±2 °C. Both the thermal strain of the mixes after each cycle and their latent strains after the test are detailed in Fig. 8.

Different stages could be distinguished in the thermal-strain patterns throughout the wet-dry test, some of which coincided with those related to the internal damage, which was evaluated through weight (Fig. 6) and UPV (Fig. 7) variations. Each stage was the same for all the mixtures:

- Cycles 1–2. A sharp increase in the thermal strain occurred, reaching values between 0.47 and 0.74 mm/m. The behavior in the first cycle was because the strain of the mixes was recorded for the first time. The increase from cycle 1–2 can be explained by the micro-cracking of the mixes in these first cycles [11].

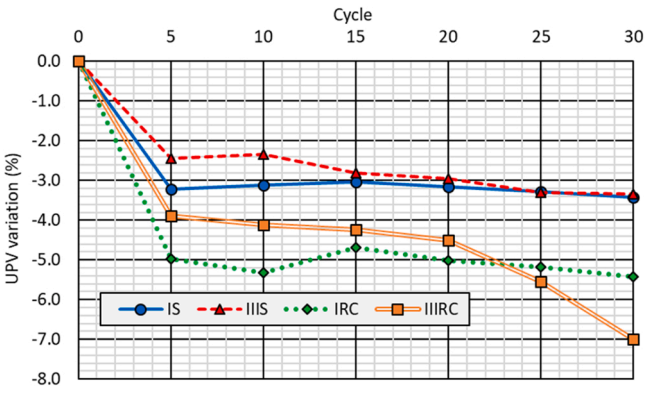

Fig. 7. UPV evolution throughout the cyclic wet-dry test.

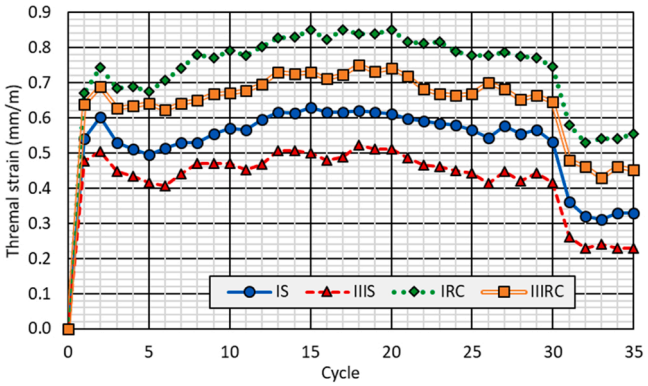

Fig. 8. Lengthening throughout the cyclic wet-dry test.

- Cycles 3–5. Thermal-strain stabilization was observed in the concrete mixtures, with some decreases even seen. It appeared that the different concrete mix components were able to adapt to temperature changes and their length remained unaffected [51], despite the internal damage recorded in the weight variations and UPV readings [65].
- Cycles 6–20. Thermal strain progressively increased in the mixes. The application of a higher number of cycles may have weakened the capability of the mixtures to withstand the thermal variations [58]. Furthermore, all the mixes showed maximum strains between 0.02 and 0.05 mm/m higher than those recorded in cycle 2, which could be a symptom of the micro-cracking that they experienced at the beginning of the test [37]. This micro-cracking separated the cementitious matrix, which resulted in an apparent increase in thermal strain [64].
- Cycles 21–30. The mixtures underwent progressive shrinking of around 0.1 mm/m. That shrinking corresponded to the cycles where a delayed increase in weight was observed as a result of concrete aging [15] and partial primary-ettringite decomposition [62]. The highest level of shrinking was reached in the *IIIRC* mix, which experienced the largest internal damage at this stage as a result of the lower quality of its cementitious matrix [11]. In a similar study on concrete performance under cyclic thermal variations, the authors found that RCA mixes underwent progressive shrinking throughout the whole test, although no water immersion tests were conducted in that study [58]. In this research, shrinking was observed from cycle 20 onwards, perhaps because immersion in water slowed down the whole shrinking process [62].

After completion of the wet-dry test, the specimens were held in the laboratory environment at 20±2 °C over an equivalent time to the duration of 5 cycles. It was found that all the mixtures showed latent strain, which was approximately 0.2 mm/m less than the thermal strain after the last cycle of the test. A behavior that was attributable to both internal damage and aging of the specimens during this test [15].

Regarding the effect of each modification on the mix composition, a direct relationship was observed between the weight variations (Fig. 6) and thermal strains (Fig. 8). On the one hand, RCA led to higher thermal deformability than EAFS. EAFS may, if not conveniently stabilized before its addition to a concrete mixture, undergo expansive trends when exposed to high temperatures [60]. In this study, adequate weathering had been performed, as indicated in the description of the raw materials, so no undue expansivity occurred. Thus, the RCA mixes presented higher deformability for three reasons: the presence of adhered mortar [18], the higher porosity levels of RCA concrete [26], and its lower thermal inertia than concretes containing EAFS, a steelmaking byproduct produced at high temperatures [24]. On the other hand, the GGBS contained in CEM III/A reduced the thermal deformability of the mixes by approximately 0.10–0.15 mm/m, as it caused a more compact micro-structure that reduced concrete deformation by up to 18% in other studies [42]. The mix composition did not change the thermal-strain evolution throughout the wet-dry test, as the strain differences between the mixes were the same throughout the whole test.

The linear thermal expansion coefficient can be calculated as the ratio between the thermal-strain values and the temperature increase (50 °C) [51,52]. Table 5 shows the 95%-confidence intervals of this coefficient during the test, in which the coefficients were notably higher in the RCA and CEM I mixes, in agreement with the explanations on the effects of mix-composition changes. The usual value of $1{\cdot}10^{-5}$ °C^{-1} was only valid for the *IIIS* mix, while higher values should be used for the other mixes, to cover the maximum

Table 5
Linear thermal expansion coefficient.

Mix	95%-confidence interval (°C^{-1})	Medium value (°C^{-1})
IS	(1.12; 1.17)	1.145
IIIS	(0.90; 0.95)	0.925
IRC	(1.52; 1.60)	1.560
IIIRC	(1.33; 1.39)	1.360

All the values are multiplied by 10^5.

strains that can arise. A value of $1.6{\cdot}10^{-5}$ °C^{-1} was sufficient for safe estimates of the maximum recorded strains, regardless of concrete composition. That maximum value was higher than the value of $1.2{\cdot}10^{-5}$ °C^{-1} found in previous investigations of the authors [58], which is explainable when the behavior of the concrete produced at full scale rather than at laboratory scale is considered [48].

4.4. Hardened-property variations

Hardened density, compressive strength, and flexural strength were measured after the wet-dry test. These results were compared with the 28-day reference values, yielding the variations shown in Fig. 9.

As discussed in previous sections, the exposure of the concrete mixes to wet-dry cycles led to approximately continuous weight increases, due to water absorption (Fig. 6), in proportion with the micro-cracking they had undergone [11]. However, their volume was also increased as found through their remaining strain (Fig. 8). Both aspects affected hardened density. In this case, the hardened density of all the mixtures presented a positive variation (increase), as shown in Fig. 9a, which was between 0.75% and 1.35%. The increase in weight was more noticeable than the increase in volume in all cases. Moreover, these variations were in accordance with what has been described above, so the density increase was higher in the RCA and CEM I mixes, because of their higher levels of porosity and internal damage throughout the test [26,33].

The variations of both compressive strength and flexural strength are detailed in Fig. 9b. Both strengths decreased in all cases as a result of internal damage, with reductions between 15% and 30%, approximately. The percentage decrease in compressive strength was slightly higher, 3–5% in absolute terms, than the percentage decrease of flexural strength, perhaps because the micro-cracking caused no great change in tensile behavior [30,64]. Regarding the effect of concrete composition, on the one hand, the mixtures with EAFS showed smaller strength decreases than the RCA mixes. RCA additions weakened the ITZ, leading to higher levels of internal damage, which resulted in higher porosity levels [18,60]. Besides, the more compact micro-structures of GGBS reduced the strength loss in combination with EAFS when compared with ordinary Portland cement [42]. However, the strength decrease in the *IIIRC* mix was slightly higher than in the *IRC* mix, in all likelihood as a result of the poorer cementitious matrix of the *IIIRC* mix, as discussed above. Thus, although its internal-damage level was lower, concrete strength was more noticeably affected [15].

4.5. Flexural deformability

Mixture stiffness before and after the wet-dry test was assessed through the load-deflection curves, as shown in Fig. 10. It was decided to evaluate that concrete characteristic, because many concrete elements that are openly exposed to wet-dry cycles, such as slabs or pavements, work mainly under bending-tensile conditions [3,13].

The load-deflection curves (Fig. 10) were standard in all the mixes [51,52]. Thus, the curves were approximately horizontal around loads equal to zero and subsequently their slopes began to increase until reaching a linear ascending section up until failure. The slope of this linear section, known as compliance, represents the stiffness of the concrete under bending-tensile loading [53], and was calculated as the slope of the least-squares fitted line to this linear section. Brittle failure occurred, as was to be expected in the absence of fibers, with the mixtures showing no increase in deflection once the maximum load had been reached [15]. Thus, the area under the curve represented the energy absorbed during the deformation process and was a measure of concrete ductility, for whose calculation the fitted line for the linear section was considered. The only mix that showed a minor difference in the curve shape was the *IRC* mix after the wet-dry test, which had a longer initial horizontal section, perhaps because of the tendency of the specimens to succumb to cracking [53]. The key parameters of the load-deflection curves are detailed in Table 6.

According to the 28-day load-deflection curves (Fig. 10a and Table 6), all the mixes had a similar flexural stiffness before the wet-dry test (compliance between 0.0311 and 0.0362 mm/kN), although the RCA mixes were less compliant because of its increased tendency to crack [30], especially the *IIIRC* mix. After the wet-dry test (Fig. 10b and Table 6), the compliance values of all the mixes increased due to the internal damage in the cementitious matrix [10,58]. The compliances of the *IIIS*, *IRC* and *IIIRC* mixes were also practically identical, at around 0.0450 mm/kN. Nevertheless, the *IS* mix showed higher deformability than the other mixes (compliance of 0.0741 mm/kN), which the low LFS content can in all likelihood explain, the effects of which had been altered after

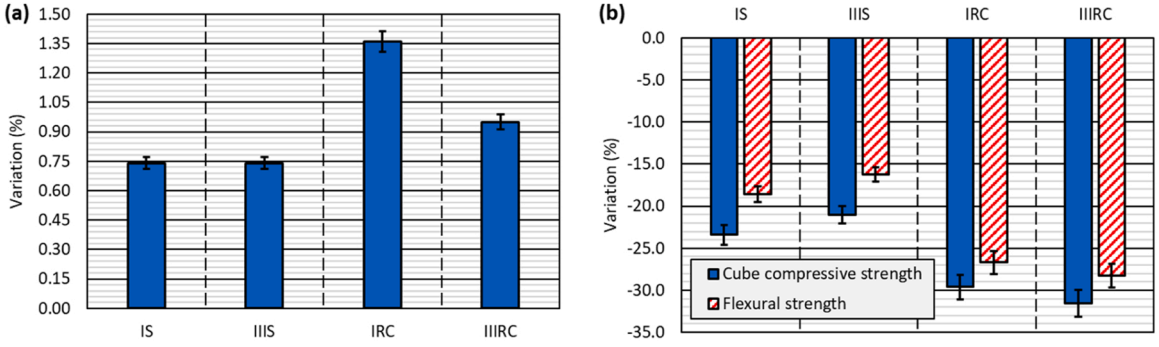

Fig. 9. Variations of the hardened properties following the cyclic wet-dry test: (a) hardened density; (b) mechanical strengths.

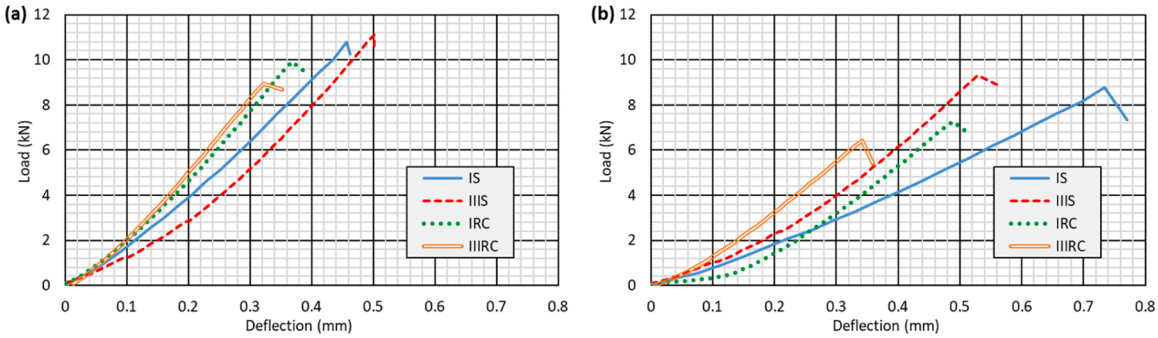

Fig. 10. Load-deflection curves: (a) before the wet-dry test (age of 28 days); (b) after the wet-dry test.

Table 6
Key values of the load-deflection performance of the mixes.

Mix		*IS*	*IIIS*	*IRC*	*IIIRC*
Compliance (mm/kN)	**Before wet-dry test**	0.0362	0.0332	0.0327	0.0311
	After wet-dry test	0.0741	0.0433	0.0475	0.0460
Failure deflection (mm)	**Before wet-dry test**	0.46	0.50	0.37	0.32
	After wet-dry test	0.73	0.53	0.49	0.34
Absorbed energy (mm·kN)	**Before wet-dry test**	2.67	2.29	1.81	1.54
	After wet-dry test	3.19	2.29	1.48	1.07

exposure to high temperatures [36,60]. It was the only aspect analyzed during the wet-dry test, in which a clear influence of this component of the mix was noted. Such a remarkable increase in deformability was not as detectable in the *IRC* mix, because its higher internal micro-cracking during the wet-dry test to a greater extent conditioned its subsequent behavior [64].

The higher deformability of the *IS* mix, together with its high flexural strength, meant that it had the highest energy-absorption capacity [15]. In the other mixes, the factor that conditioned energy absorption, at equal compliance, was flexural strength: the higher the flexural strength, the greater the absorbed energy. Similarly, the flexural strength of all the mixtures also conditioned their failure deflection, higher strengths implying delayed ductile failure. Analyzing the effect of the wet-dry cycles, the decrease in flexural strength was more noticeable than the increase in both compliance and failure deflection, which led to lower absorbed energy after wet-dry aging in the RCA mixes. The lower reduction in flexural strength and the higher increase in compliance in the EAFS mixes caused that the energy absorption remained constant or even increased after the wet-dry test, thus EAFS mixes exhibiting a performance similar to that found in other studies [11,60].

4.6. Statistical validation

The significance of the results throughout the wet-dry tests was evaluated with a two-way ANalysis Of VAriance (ANOVA) at a 95%-confidence level by considering the three experimental results for each property and concrete mix. The objective was to analyze the dispersion of the results obtained in the different specimens tested for each mix, thus evaluating the significance of the factors considered in this research (aggregate type and cement type). The *p*-values obtained for each property regarding the effect of the factors and their interaction are detailed in Table 7.

According to these *p*-values, it can be appreciated that the aggregate type always significantly affected all the dimensions of wet-dry behavior. In fact, aggregate type had the highest influence upon all the samples, except for compliance, in view of the different deformational responses of the *IS* and *IIIS* mixes after the test. With regard to the cement type, no significant effect was evidenced in the hardened-property variations or in compliance. That behavior was mainly because of the different effects of the cement type, depending on the type of aggregate with which it was combined, mainly because of the low quality cementitious matrix of the *IIIRC* mix [11]. Finally, the interaction between both factors was only significant regarding strength variations, which showed that each different combination of wastes resulted in a different strength after the wet-dry test.

4.7. Multi-criteria mix selection

A Multi-Criteria Decision-Making (MCDM) analysis with the purpose of objectively defining the best mix behavior after exposure to the wet-dry cycles was conducted. TOPSIS and PROMETHEE algorithms, which are commonly used MCDM tools for the analysis of construction materials [20,67,68], were used. On the one hand, the TOPSIS algorithm allows the determination of the optimal choice alternative by comparing each alternative with the best and worst combination of choice criteria [67]. On the other hand, the PROMETHEE algorithm determines the optimal choice alternative through a comparison of all the alternatives for each individual choice criterion [20]. The five dimensions analyzed in relation to wet-dry behavior (weight, UPV, strain, hardened-property variations,

Table 7
p-values of the two-way 95%-confidence ANOVA.

Property	Aggregate type	Cement type	Interaction
Final weight increase	0.0001	0.0191	0.2341
Final lower UPV reading	0.0000	0.0017	0.0612
Final length increase	0.0004	0.0057	0.7096
Remaining strain	0.0004	0.0075	0.9963
Hardened-density variation	0.0043	0.1097	0.1097
Compressive-strength variation	0.0000	0.1230	0.0000
Flexural-strength variation	0.0000	0.1161	0.0000
Compliance	0.0445	0.2679	0.3477
Failure deflection	0.0004	0.0009	0.2794
Absorbed energy	0.0001	0.0028	0.0704

and flexural deformability) were considered as choice criteria, all of them of equal importance (weight of 20%). Thus, a multi-purpose mix selection was conducted [49]. Nevertheless, some dimensions involved several quantities. For example, the dimension *"hardened-property variations"* incorporated three quantities: hardened-density variation, compressive-strength variation, and flexural-strength variation. In those cases, all the quantities were considered equally important. The ranking of mixtures shown in Fig. 11 was obtained in that way.

The MCDM analysis showed that, according to both algorithms, the EAFS mixes had better overall performance, so they might well be the most suitable in applications where there is significant exposure to cyclic wet-dry phenomena. The *IIIS* mix was positioned in the first place as the most suitable mix, as a result of its lower internal-damage level, lower thermal strain, and lower strength and stiffness decreases, and its more compact micro-structure, as a result of the presence of GGBS [42,44]. The choice between both RCA mixes would be indifferent according to the average-ranking criterion (Fig. 11b), as their positions were either 3 or 4 depending on the MCDM algorithm. It shows that the use of GGBS in full-scale mixes never modified the performance obtained with ordinary Portland cement when combined with RCA [48]. Thus, RCA conditioned the concrete behavior throughout the wet-dry tests to a greater extent than the cement type.

5. Conclusions

The behavior under wet-dry cycles of high-workability green concretes produced at full scale (0.5-m^3 volume) has been analyzed in this paper. These mixtures incorporated large amounts of sustainable raw materials, such as Electric Arc Furnace Slag (EAFS) and Recycled Concrete Aggregate (RCA) as aggregates, and Ladle Furnace Slag (LFS) and Ground Granulated Blast-furnace Slag (GGBS) as binders. The concrete mixes were subjected to 30 cycles of 16 hours of water immersion at 20±2 °C and 8 hours of oven-drying at 70 ±2 °C. The objective was to validate the use of these mixtures when produced in industrial volumes and exposed to intermittent rain and solar heating. The following conclusions can be drawn from the overall results:

- The EAFS mixes performed better than the other mixes, showing lower weight increases due to water absorption that implied less internal damage and micro-cracking in the wet-dry tests. A behavior that was even improved following the addition of GGBS that contributed to more compact concrete micro-structures. As common in concrete, all the mixes experienced the most significant internal damage in the early wet-dry cycles regardless of their composition, although some internal damage because of long-term aging of the cementitious matrix was also detected.
- Ultrasonic Pulse Velocity (UPV) test results corroborated the internal damage to the concrete. This indirect measure showed that the combination of fine RCA and GGBS was inadequate, as the internal damage as a result of the aging of the mixes prepared with both wastes was considerably higher. Such large levels of internal damage were not detected from the weight increase.

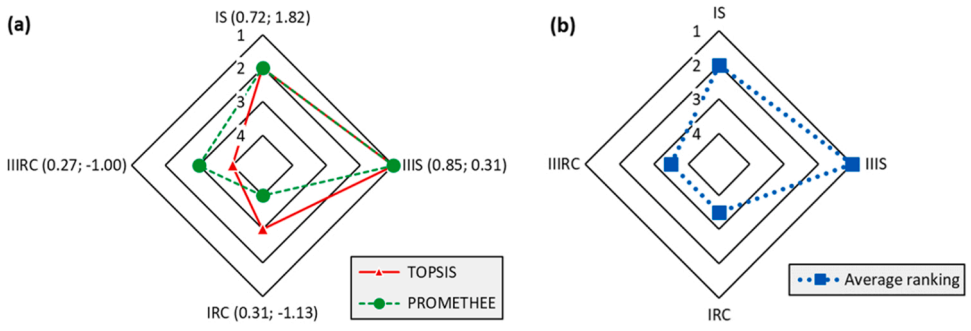

Fig. 11. Ranking of mixes with regard their cyclic wet-dry performance: (a) individual results of algorithms (relative-closeness coefficient according to the TOPSIS algorithm; net flow as *per* the PROMETHEE algorithm); (b) average ranking.

- All the mixes underwent expansion in the presence of rising temperatures. The strain levels increased in the early cycles together with micro-cracking, while the mixes underwent long-term shrinking, as the cementitious matrix aged. EAFS and GGBS reduced the thermal-strain levels, in part because of the lower internal damage of the mixtures that incorporated them, which also resulted in lower latent strain. The maximum thermal strain of the concretes, regardless of their compositions, could be safely estimated with a linear thermal expansion coefficient of $1.6{\cdot}10^{-5}$ $^{\circ}C^{-1}$.
- The hardened densities of all the mixes increased around 1% after the wet-dry test, due to water absorption. On the other hand, compressive and flexural strengths decreased between 15% and 30%. The EAFS mixes experienced the lowest strength losses, but the effect of GGBS was not as pronounced, as the concrete mixes showed very similar strength decreases, regardless of the binder type.
- The mix composition had no appreciable effects on the flexural deformability of the concrete mixtures following their exposure to wet-dry cycles, as compliance was similar in all the mixtures. The mix made with EAFS, ordinary Portland cement, and LFS showed a slightly higher deformability, perhaps as a result of expansive phenomena and thermal alteration of the LFS.

In statistical language, each change in mix composition significantly affected the behavior of high-workability concrete under wet-dry cycles. An observation that underlines the need for careful study of concrete mix design for components that exposed to wet environments. It was noted in the multi-criteria analysis with a multi-purpose approach that a combination of EAFS with GGBS presented the best overall performance and was the best choice for high-workability applications. On the contrary, the use of RCA was not thought to be recommendable, all the more so as the cyclic wet-dry behavior of the RCA mixtures showed no improvement after the addition of GGBS.

CRediT authorship contribution statement

Víctor Revilla-Cuesta: Writing – original draft, Validation, Methodology, Investigation, Formal analysis, Data curation, Conceptualization. **Javier Manso-Morato:** Writing – review & editing, Visualization, Software, Methodology, Investigation, Formal analysis. **Nerea Hurtado-Alonso:** Writing – review & editing, Visualization, Software, Methodology, Investigation, Formal analysis. **Amaia Santamaría:** Writing – review & editing, Supervision, Software, Methodology, Investigation, Conceptualization. **José T. San-José**: Writing – review & editing, Supervision, Resources, Project administration, Funding acquisition, Conceptualization.

Declaration of Competing Interest

The authors declare that they have no known competing financial interests or personal relationships that could have appeared to influence the work reported in this paper.

Data availability

All data generated are included in the paper, since this research is of an experimental nature. The authors are available for any further clarification.

Acknowledgements

This research work was supported by the Spanish Ministry of Universities, MICINN, AEI, EU, “ERDF A way of making Europe”, by the “European Union” and NextGenerationEU/PRTR [grant numbers PID2020-113837RB-I00; PID2021-124203OB-I00; PID2023-146642OB-I00; 10.13039/501100011033; TED2021-129715B-I00; FPU21/04364]; the Junta de Castilla y León (Regional Government) and ERDF [grant number UIC-231; BU033P23; BU066-22]; the Basque Government [IT1619-22 SAREN research group]; and, finally, the University of Burgos [grant number SUCONS, Y135.GI].

References

[1] S.T. Deresa, J. Xu, C. Demartino, Y. Heo, Z. Li, Y. Xiao, A review of experimental results on structural performance of reinforced recycled aggregate concrete beams and columns, Adv. Struct. Eng. 23 (15) (2020) 3351–3369, https://doi.org/10.1177/1369433220934564.
[2] Z. Dong, T. Han, B. Zhang, H. Zhu, G. Wu, Y. Wei, P. Zhang, A review of the research and application progress of new types of concrete-filled FRP tubular members, Constr. Build. Mater. 312 (2021) 125353, https://doi.org/10.1016/j.conbuildmat.2021.125353.
[3] R. Joumblat, Z. Al Basiouni Al Masri, G. Al Khateeb, A. Elkordi, A.R. El Tallis, J. Absi, State-of-the-art review on permanent deformation characterization of asphalt concrete pavements, Sustainability 15 (2) (2023) 1166, https://doi.org/10.3390/su15021166.
[4] E. Sengun, S. Kim, H. Ceylan, A comparative study on structural design of plain and roller-compacted concrete for heavy-duty pavements, Road. Mater. Pavement Des. 25 (2) (2024) 392–442, https://doi.org/10.1080/14680629.2023.2209194.
[5] F. Özalp, Effects of electric arc furnace (EAF) slags on mechanical and permeability properties of paving stone, kerb and concrete pipes, Constr. Build. Mater. 329 (2022) 127159, https://doi.org/10.1016/j.conbuildmat.2022.127159.
[6] M. Javadi, R. Hassanli, M.M. Rahman, M.R. Karim, Behaviour of self-centring shear walls—a state of the art review, Front. Struct. Civ. Eng. 17 (1) (2023) 53–77, https://doi.org/10.1007/s11709-022-0850-0.
[7] F. Fiol, V. Revilla-Cuesta, C. Thomas, J.M. Manso, Self-compacting concrete containing coarse recycled precast-concrete aggregate and its durability in marine-environment-related tests, Constr. Build. Mater. 377 (2023) 131084, https://doi.org/10.1016/j.conbuildmat.2023.131084.
[8] J. Guo, X. Xia, K. Wang, Y. Xu, Multi-scale model investigating the effects of pore structure and drying-wetting cycles on diffusion in concrete, Cem. Concr. Compos. 140 (2023) 105086, https://doi.org/10.1016/j.cemconcomp.2023.105086.

[9] A. Beglarigale, H. Yiğiter, H. Yazlcl, Corrosion performance of various reinforced concretes subjected to a systematic wetting-drying cycle regime in real marine environment, J. Mater. Civ. Eng. 35 (5) (2023) 04023056, https://doi.org/10.1061/(ASCE)MT.1943-5533.0004707.
[10] H. Jin, X. Fan, Z. Li, W. Zhang, J. Liu, D. Zhong, L. Tang, An experimental study on the influence of continuous ambient humidity conditions on relative humidity changes, chloride diffusion and microstructure in concrete, J. Build. Eng. 59 (2022) 105112, https://doi.org/10.1016/j.jobe.2022.105112.
[11] V. Ortega-López, F. Faleschini, C. Pellegrino, V. Revilla-Cuesta, J.M. Manso, Validation of slag-binder fiber-reinforced self-compacting concrete with slag aggregate under field conditions: durability and real strength development, Constr. Build. Mater. 320 (2022) 126280, https://doi.org/10.1016/j.conbuildmat.2021.126280.
[12] C.H. Lin, W.C. Lin, S.T. Chen, Shear behaviour of prestressed beams with high-workability concrete, Mag. Concr. Res. 64 (5) (2012) 419–432, https://doi.org/10.1680/macr.10.00203.
[13] O. Smirnova, Concrete mixtures with high-workability for ballastless slab tracks, J. King Saud. Univ. Eng. Sci. 29 (4) (2017) 381–387, https://doi.org/10.1016/j.jksues.2017.06.004.
[14] I. González-Taboada, B. González-Fonteboa, J. Eiras-López, G. Rojo-López, Tools for the study of self-compacting recycled concrete fresh behaviour: workability and rheology, J. Clean. Prod. 156 (2017) 1–18, https://doi.org/10.1016/j.jclepro.2017.04.045.
[15] V. Ortega-López, V. Revilla-Cuesta, A. Santamaría, A. Orbe, M. Skaf, Microstructure and dimensional stability of slag-based high-workability concrete with steelmaking slag aggregate and fibers, J. Mater. Civ. Eng. 34 (9) (2022) 04022224, https://doi.org/10.1061/(ASCE)MT.1943-5533.0004372.
[16] R.A. Schankoski, P.R. de Matos, R. Pilar, L.R. Prudêncio Jr., R.D. Ferron, Rheological properties and surface finish quality of eco-friendly self-compacting concretes containing quarry waste powders, J. Clean. Prod. 257 (2020) 120508, https://doi.org/10.1016/j.jclepro.2020.120508.
[17] EN-Euronorm, Rue de stassart, 36. Belgium-1050 Brussels, European Committee for Standardization.
[18] S. Malazdrewicz, K.Adam Ostrowski, Sadowski, Self-compacting concrete with recycled coarse aggregates from concrete construction and demolition waste – Current state-of-the art and perspectives, Constr. Build. Mater. 370 (2023) 130702, https://doi.org/10.1016/j.conbuildmat.2023.130702.
[19] P. Zhang, S. Wei, G. Cui, Y. Zhu, J. Wang, Properties of fresh and hardened self-compacting concrete incorporating rice husk ash: a review, Rev. Adv. Mater. Sci. 61 (1) (2022) 563–575, https://doi.org/10.1515/rams-2022-0050.
[20] V. Revilla-Cuesta, F. Fiol, P. Perumal, V. Ortega-López, J.M. Manso, Using recycled aggregate concrete at a precast-concrete plant: a multi-criteria company-oriented feasibility study, J. Clean. Prod. 373 (2022) 133873, https://doi.org/10.1016/j.jclepro.2022.133873.
[21] L.J. Drew, W.H. Langer, J.S. Sachs, Environmentalism and natural aggregate mining, Nat. Resourc. Res. 11 (1) (2002) 19–28, https://doi.org/10.1023/A:1014283519471.
[22] A. Aghajanian, A. Cimentada, M. Fayyaz, A.S. Brand, C. Thomas, ITZ microanalysis of cement-based building materials with incorporation of siderurgical aggregates, J. Build. Eng. 67 (2023) 106008, https://doi.org/10.1016/j.jobe.2023.106008.
[23] F. Faleschini, M.A. Zanini, K. Toska, Seismic reliability assessment of code-conforming reinforced concrete buildings made with electric arc furnace slag aggregates, Eng. Struct. 195 (2019) 324–339, https://doi.org/10.1016/j.engstruct.2019.05.083.
[24] A.M. Rashad, Behavior of steel slag aggregate in mortar and concrete - a comprehensive overview, J. Build. Eng. 53 (2022) 104536, https://doi.org/10.1016/j.jobe.2022.104536.
[25] H. Qasrawi, Hardened properties of green self-consolidating concrete made with steel slag coarse aggregates under hot conditions, Acids Mater. J. 117 (1) (2020) 107–118, https://doi.org/10.14359/51719072.
[26] A. Piccinali, A. Diotti, G. Plizzari, S. Sorlini, Impact of recycled aggregate on the mechanical and environmental properties of concrete: a review, Materials 15 (5) (2022) 1818, https://doi.org/10.3390/ma15051818.
[27] C. Vintimilla, M. Etxeberria, Limiting the maximum fine and coarse recycled aggregates-type a used in structural concrete, Constr. Build. Mater. 380 (2023) 131273, https://doi.org/10.1016/j.conbuildmat.2023.131273.
[28] A. Santamaría, A. Orbe, M.M. Losañez, M. Skaf, V. Ortega-Lopez, J.J. González, Self-compacting concrete incorporating electric arc-furnace steelmaking slag as aggregate, Mater. Des. 115 (2017) 179–193, https://doi.org/10.1016/j.matdes.2016.11.048.
[29] G. Adegoloye, A.L. Beaucour, S. Ortola, A. Noumowe, Mineralogical composition of EAF slag and stabilised AOD slag aggregates and dimensional stability of slag aggregate concretes, Constr. Build. Mater. 115 (2016) 171–178, https://doi.org/10.1016/j.conbuildmat.2016.04.036.
[30] H. Liu, J. Xiao, T. Ding, Flexural performance of 3D-printed composite beams with ECC and recycled fine aggregate concrete: experimental and numerical analysis, Eng. Struct. 283 (2023) 115865, https://doi.org/10.1016/j.engstruct.2023.115865.
[31] J.A. Forero, J. de Brito, L. Evangelista, C. Pereira, Improvement of the quality of recycled concrete aggregate subjected to chemical treatments: a review, Materials 15 (8) (2022) 2740, https://doi.org/10.3390/ma15082740.
[32] F. Rodrigues, L. Evangelista, J.D. Britoa, A new method to determine the density and water absorption of fine recycled aggregates, Mater. Res. 16 (5) (2013) 1045–1051, https://doi.org/10.1590/S1516-14392013005000074.
[33] S. Santos, P.R. da Silva, J. de Brito, Self-compacting concrete with recycled aggregates – a literature review, J. Build. Eng. 22 (2019) 349–371, https://doi.org/10.1016/j.jobe.2019.01.001.
[34] D.L. Tran, M. Mouret, F. Cassagnabère, Impact of the porosity and moisture state of coarse aggregates, and binder nature on the structure of the paste-aggregate interface: elementary model study, Constr. Build. Mater. 319 (2022) 126112, https://doi.org/10.1016/j.conbuildmat.2021.126112.
[35] K.K. Sideris, C. Tassos, A. Chatzopoulos, P. Manita, Mechanical characteristics and durability of self compacting concretes produced with ladle furnace slag, Constr. Build. Mater. 170 (2018) 660–667, https://doi.org/10.1016/j.conbuildmat.2018.03.091.
[36] A. Rodríguez, I. Santamaría-Vicario, V. Calderón, C. Junco, J. García-Cuadrado, Study of the expansion of cement mortars manufactured with Ladle Furnace Slag LFS, Mater. Constr. 69 (334) (2019) e183, https://doi.org/10.3989/mc.2019.06018.
[37] S. Lian, T. Meng, Y. Zhao, Z. Liu, X. Zhou, S. Ruan, Experimental and theoretical analyses of chloride transport in recycled concrete subjected to a cyclic drying-wetting environment, Structures 52 (2023) 1020–1034, https://doi.org/10.1016/j.istruc.2023.04.036.
[38] G. Kaplan, J. Shi, A. Öz, B. Bayrak, M.H. Dheyaaldin, A.C. Aydın, Preparation and characterization of a novel prepacked aggregate geopolymer: a feasibility study, Powder Technol. 421 (2023) 118423, https://doi.org/10.1016/j.powtec.2023.118423.
[39] C.O. Nwankwo, G.O. Bamigboye, I.E.E. Davies, T.A. Michaels, High volume Portland cement replacement: a review, Constr. Build. Mater. 260 (2020) 120445, https://doi.org/10.1016/j.conbuildmat.2020.120445.
[40] S. Parathi, P. Nagarajan, S.A. Pallikkara, Ecofriendly geopolymer concrete: a comprehensive review, Clean. Technol. Environ. Policy 23 (6) (2021) 1701–1713, https://doi.org/10.1007/s10098-021-02085-0.
[41] V. Revilla-Cuesta, M. Skaf, A. Santamaría, J.J. Hernández-Bagaces, V. Ortega-López, Temporal flowability evolution of slag-based self-compacting concrete with recycled concrete aggregate, J. Clean. Prod. 299 (2021) 126890, https://doi.org/10.1016/j.jclepro.2021.126890.
[42] J.R. Weng, W.C. Liao, Microstructure and shrinkage behavior of high-performance concrete containing supplementary cementitious materials, Constr. Build. Mater. 308 (2021) 125045, https://doi.org/10.1016/j.conbuildmat.2021.125045.
[43] Y.J. Du, J. Wu, Y.L. Bo, N.J. Jiang, Effects of acid rain on physical, mechanical and chemical properties of GGBS–MgO-solidified/stabilized Pb-contaminated clayey soil, Acta Geotech. 15 (4) (2020) 923–932, https://doi.org/10.1007/s11440-019-00793-y.
[44] J. Pacheco, R.B. Polder, Critical chloride concentrations in reinforced concrete specimens with ordinary Portland and blast furnace slag cement, Heron 61 (2) (2016) 99–119.
[45] M. Elsayed, B.A. Tayeh, Y.I. Abu Aisheh, N.A. El-Nasser, M.A. Elmaaty, Shear strength of eco-friendly self-compacting concrete beams containing ground granulated blast furnace slag and fly ash as cement replacement, Case Stud. Constr. Mater. 17 (2022) e01354, https://doi.org/10.1016/j.cscm.2022.e01354.
[46] R. Shamass, O. Rispoli, V. Limbachiya, R. Kovacs, Mechanical and GWP assessment of concrete using blast furnace slag, silica fume and recycled aggregate, Case Stud. Constr. Mater. 18 (2023) e02164, https://doi.org/10.1016/j.cscm.2023.e02164.
[47] J. Cao, Z. Jin, Q. Ding, C. Xiong, G. Zhang, Influence of the dry/wet ratio on the chloride convection zone of concrete in a marine environment, Constr. Build. Mater. 316 (2022) 125794, https://doi.org/10.1016/j.conbuildmat.2021.125794.

[48] A. Santamaría, V. Revilla-Cuesta, M. Skaf, J.M. Romera, Full-scale sustainable structural concrete containing high proportions of by-products and waste, Case Stud. Constr. Mater. 18 (2023) e02142, https://doi.org/10.1016/j.cscm.2023.e02142.
[49] V. Revilla-Cuesta, M. Skaf, A.B. Espinosa, V. Ortega-López, Multi-criteria feasibility of real use of self-compacting concrete with sustainable aggregate, binder and powder, J. Clean. Prod. 325 (2021) 129327, https://doi.org/10.1016/j.jclepro.2021.129327.
[50] M. Nepomuceno, L. Oliveira, Parameters for self-compacting concrete mortar phase, Am. Concr. Inst. Acids Spec. Publ. (2008) 311–327.
[51] EC-2, Eurocode 2: Design of concrete structures. Part 1-1: General rules and rules for buildings, CEN (European Committee for Standardization) (2010).
[52] ACI Committees 318M-14 and RM-14, Building code requirements for structural concrete: Farmington Hills, MI: American Concrete Institute.
[53] A. Santamaría, V. Ortega-López, M. Skaf, J.A. Chica, J.M. Manso, The study of properties and behavior of self compacting concrete containing Electric Arc Furnace Slag (EAFS) as aggregate, Ain Shams Eng. J. 11 (1) (2020) 231–243, https://doi.org/10.1016/j.asej.2019.10.001.
[54] UNE 83966, Concrete durability. Test methods. Conditioning of concrete test pieces for the purpose of gas permeability and capilar suction tests (2008).
[55] UNE 83980, Concrete durability. Test methods. Determination of the water absorption, density and accesible porosity for water in concrete (2014).
[56] ASTM-International, Book Annual of ASTM Standars, West Conshohocken, 19429–2959 2008 USA PA (2008).
[57] V. Ortega-López, J.A. Fuente-Alonso, A. Santamaría, J.T. San-José, Á. Aragón, Durability studies on fiber-reinforced EAF slag concrete for pavements, Constr. Build. Mater. 163 (2018) 471–481, https://doi.org/10.1016/j.conbuildmat.2017.12.121.
[58] V. Revilla-Cuesta, M. Skaf, J.A. Chica, J.A. Fuente-Alonso, V. Ortega-López, Thermal deformability of recycled self-compacting concrete under cyclical temperature variations, Mater. Lett. 278 (2020) 128417, https://doi.org/10.1016/j.matlet.2020.128417.
[59] M. Nepomuceno, L. Oliveira, S.M.R. Lopes, Methodology for mix design of the mortar phase of self-compacting concrete using different mineral additions in binary blends of powders, Constr. Build. Mater. 26 (1) (2012) 317–326, https://doi.org/10.1016/j.conbuildmat.2011.06.027.
[60] A.S. Brand, E.O. Fanijo, A review of the influence of steel furnace slag type on the properties of cementitious composites, Appl. Sci. 10 (22) (2020) 8210, https://doi.org/10.3390/app10228210.
[61] D. Carro-López, B. González-Fonteboa, J. De Brito, F. Martínez-Abella, I. González-Taboada, P. Silva, Study of the rheology of self-compacting concrete with fine recycled concrete aggregates, Constr. Build. Mater. 96 (2015) 491–501, https://doi.org/10.1016/j.conbuildmat.2015.08.091.
[62] P.K. Metha, P.J.M. Monteiro, 2014ISBN 978-0-07-179787-0Fourth edition, Concrete: Microstructure, properties and materials, McGraw-Hill Education2014.
[63] J. Pradhan, S. Panda, S.K. Parhi, P. Pradhan, S.K. Panigrahi, GGBFS-based self-compacting geopolymer concrete with optimized mix parameters established on fresh, mechanical, and durability characteristics, J. Mater. Civ. Eng. 36 (2) (2024) 04023578, https://doi.org/10.1061/JMCEE7.MTENG-16669.
[64] V. Revilla-Cuesta, M. Skaf, J.A. Chica, V. Ortega-López, J.M. Manso, Quantification and characterization of the microstructural damage of recycled aggregate self-compacting concrete under cyclic temperature changes, Mater. Lett. 333 (2023) 133628, https://doi.org/10.1016/j.matlet.2022.133628.
[65] M.A. Abed, B.A. Tayeh, B.H. Abu Bakar, R. Nemes, Two-year non-destructive evaluation of eco-efficient concrete at ambient temperature and after freeze-thaw cycles, Sustainability 13 (19) (2021) 10605, https://doi.org/10.3390/su131910605.
[66] R. Jones, The ultrasonic testing of concrete, Ultrasonics 1 (2) (1963) 78–82, https://doi.org/10.1016/0041-624X(63)90058-1.
[67] M. Abed, K. Rashid, M.U. Rehman, M. Ju, Performance keys on self-compacting concrete using recycled aggregate with fly ash by multi-criteria analysis, J. Clean. Prod. 378 (2022) 134398, https://doi.org/10.1016/j.jclepro.2022.134398.
[68] M. Shmlls, M. Abed, J. Fořt, T. Horvath, D. Bozsaky, Towards closed-loop concrete recycling: life cycle assessment and multi-criteria analysis, J. Clean. Prod. 410 (2023) 137179, https://doi.org/10.1016/j.jclepro.2023.137179.